Massive infection and loss of memory CD4$^+$ T cells in multiple tissues during acute SIV infection

Joseph J. Mattapallil[1], Daniel C. Douek[2], Brenna Hill[2], Yoshiaki Nishimura[3], Malcolm Martin[3] & Mario Roederer[1]

[1]*ImmunoTechnology Section and* [2]*Human Immunology Section, Vaccine Research Center, and* [3]*Laboratory of Molecular Microbiology, NIAID, NIH, Bethesda, Maryland 20892, USA*

It has recently been established that both acute human immunodeficiency virus (HIV) and simian immunodeficiency virus (SIV) infections are accompanied by a dramatic and selective loss of memory CD4$^+$ T cells predominantly from the mucosal surfaces. The mechanism underlying this depletion of memory CD4$^+$ T cells (that is, T-helper cells specific to previously encountered pathogens) has not been defined. Using highly sensitive, quantitative polymerase chain reaction together with precise sorting of different subsets of CD4$^+$ T cells in various tissues, we show that this loss is explained by a massive infection of memory CD4$^+$ T cells by the virus. Specifically, 30–60% of CD4$^+$ memory T cells throughout the body are infected by SIV at the peak of infection, and most of these infected cells disappear within four days. Furthermore, our data demonstrate that the depletion of memory CD4$^+$ T cells occurs to a similar extent in all tissues. As a consequence, over one-half of all memory CD4$^+$ T cells in SIV-infected macaques are destroyed directly by viral infection during the acute phase—an insult that certainly heralds subsequent immunodeficiency. Our findings point to the importance of reducing the cell-associated viral load during acute infection through therapeutic or vaccination strategies.

Chronic HIV infection is characterized by a steady but generally slow loss of CD4$^+$ T cells, of both naive and memory phenotypes. In contrast, the loss of CD4$^+$ T cells from peripheral blood during acute infection has been generally regarded to be modest and transient. However, studies using the SIV infection model have documented that acute infection is accompanied by a marked depletion of CD4$^+$ memory T cells primarily in mucosal tissues[1,2]; this has recently been confirmed in humans infected with HIV[3]. These studies suggest that mucosal CD4$^+$ T cells are the primary target for HIV infection and replication because of their high expression of the viral co-receptor CCR5 (ref. 4) as well as their relatively activated state[5]. Furthermore, it was observed that CD4$^+$ T cells with a mucosal homing phenotype were essentially completely absent, even from the peripheral blood[6]. As a consequence, the gut-associated mucosal tissue is viewed as the most important site of active viral replication and T-cell depletion during acute infection, owing to the concentration of viral targets at this site.

The frequency of infected CD4$^+$ T cells in the chronic phase of SIV/HIV infection is too low (0.01–1%) to account for this ongoing depletion by viral infection[7–10]. The mechanism for the massive and rapid loss during the acute phase is unknown. To answer this question, we longitudinally sampled blood, inguinal lymph nodes, as well as mucosal tissue and associated lymph nodes from the same animals before and after SIV infection at a regular and high frequency. In this way, we could address the issue of tissue distribution of T cells, a matter that clouds the interpretation of measurements taken solely from peripheral blood. Furthermore, we performed highly sensitive quantitative polymerase chain reaction (qPCR) analyses to determine which subsets of CD4$^+$ T cells were infected, and to what extent virus propagated through these subsets.

T-cell dynamics

With the objective of delineating changes in T-cell subsets during early acute infection, we longitudinally evaluated the effects of SIV infection on naive and memory T-cell subsets in blood, inguinal and mesenteric lymph nodes and jejunal mucosa, and compared them to pre-infection values (Figs 1 and 2). In nearly all animals (rhesus macaques, *Macaca mulatta*) there is an early increase in CD4$^+$ T cells at day 3 after infection in the blood (Fig. 2a). This is probably a re-distribution from other tissues, caused by an early, perhaps innate, immune response to the infection. By day 14 after infection, there is a 20% decrease in the number of CD4$^+$ T cells from the blood and lymph nodes. In contrast, as previously reported[1,2,4], the jejunum exhibits a near total loss of CD4$^+$ T cells. Notably, these losses are significantly greater than the fraction of CCR5$^+$ CD4$^+$ T cells present in these tissues.

Because CCR5, the SIV co-receptor[11,12], is expressed solely on memory CD4$^+$ T cells, we hypothesized that quantifying memory subset dynamics would provide a better view of the ongoing infection. As shown in Fig. 1a, naive T cells in these animals typically comprise 50–75% of T cells in blood (in adult humans this averages 50%). Consequently, the dynamics of CD4$^+$ memory T cells are far more marked than for the total compartment. An early expansion (day 3) is followed by the loss of 60–80% of memory T cells. This loss is seen in multiple tissues, although it appears first in the blood and lymph nodes and a few days later in the jejunum[1,2]. Thus, the SIV-induced depletion of CD4$^+$ T cells during acute infection is not principally restricted to T cells of mucosal origin. However, in terms of the total number of CD4$^+$ T cells lost from an animal, most are from the mucosa, as the greatest number of T cells are resident there.

We quantified the CCR5-expressing T cells in the various tissues. As previously described[4,6], these cells disappear quickly from the peripheral blood—beginning before the onset of viraemia. Interestingly, even CCR5$^+$ CD8$^+$ T cells were found to disappear from the blood; however, unlike CCR5$^+$ CD4$^+$ T cells, they continued to be found in other tissues.

Viral dynamics

In order to understand the role of viral infection of CD4$^+$ T cells on their dynamics, we quantified both plasma and cell-associated virus (Fig. 3). We used qPCR[7] on bulk-sorted subsets of T cells to

determine the extent to which direct SIV infection could account for the loss of memory CD4$^+$ T cells. Starting shortly after infection, the number of SIV-Gag copies in memory CD4$^+$ T-cell subsets rose steadily, peaking at day 10 after infection in all tissues examined (Fig. 3b). In fact, at peak, we observed a very high number of SIV-Gag copies (50–200,000 per 10^5 CD4$^+$ memory T cells). The level of SIV-Gag copies then declined dramatically by day 14 after infection (Fig. 3b). These kinetics reflect the highly dynamic nature of the infection, and underscore the importance of measuring parameters of infection at the infection peak (day 10–11 after infection) as well as after the peak.

The amount of SIV-Gag DNA in memory CD4$^+$ T cells correlated well with the plasma viral loads (Fig. 3c), similar to what has been shown for the chronic phase of HIV infection in humans[7]. This suggests that plasma virus arises directly from infected memory CD4$^+$ T cells.

The high levels of SIV-Gag DNA could be due to a very high number of copies in a small number of cells, or to a low number of copies in nearly all memory cells. To distinguish between these possibilities, we quantified the amount of SIV-Gag DNA in single-sorted memory T cells (Table 1). We calibrated our results using a cell line carrying a single copy of proviral DNA. We thus determined that CD4$^+$ memory T cells in all the tissues examined carried, on average, 1.5 copies of Gag DNA (Table 1). This measurement is in good agreement with published data for HIV infection in humans, where infected CD4$^+$ T cells in lymph nodes carried on average two copies of viral DNA[13,14]. From the quantification of Gag DNA at the single cell level, we could determine that the fraction of cells infected in the different tissues (Table 1) ranged from 30 to 60% of all memory CD4$^+$ T cells at the peak of infection.

Quantification of viral load in purified naive T cells confirmed the intrinsic resistance of these cells to SIV infection[15]. On the basis of qPCR of 168 wells of single- or low-number cell sorts, we estimate that less than 0.5% (1 out of 200) of naive T cells were infected by SIV even at day 10 after infection (data not shown).

By day 14, the cell-associated viral load in all tissues dropped about 80% from peak values. Because this viral load is quantified by the presence of Gag DNA, the loss corresponds to the loss of 80% of infected CD4$^+$ T cells. Because we found similar kinetics in all tissues, we do not believe that a redistribution of cells accounts for this loss.

Apparent CCR5 expression does not correlate with infection

SIV uses CCR5 as its co-receptor[11,12]; the lack of expression of CCR5 by naive T cells presumably underlies their resistance to SIV infection. However, the infection rate in the tissues described above (30–60%) far exceeds the well-described expression of CCR5 by memory T cells in these tissues as well as the rate that we found for our animals (~3% of total CD4$^+$ T cells in peripheral blood and lymph nodes, ~50% in mucosa; Fig. 1).

We determined that the ability to measure CCR5 expression by flow cytometry does not correlate with the presence of SIV in memory CD4$^+$ T cells. The level of viral infection in sorted CCR5$^+$ cells was essentially the same as that for sorted CCR5$^-$ cells (Fig. 3b). We hypothesized that CCR5$^-$ memory T cells are not truly negative for CCR5 expression—they simply do not express enough receptor to be detectable by flow cytometry. To address this, we quantified CCR5 messenger RNA expression on sorted naive, CCR5$^-$ and

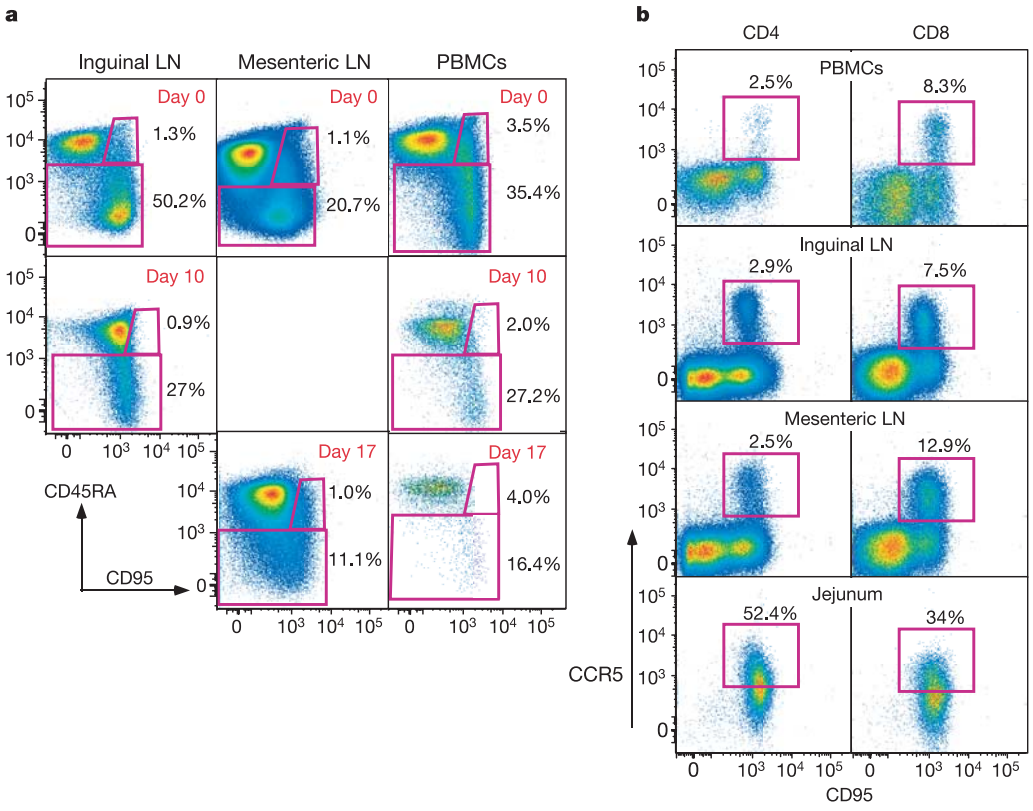

Figure 1 Identification of subsets of CD4$^+$ and CD8$^+$ T cells in a non-human primate (rhesus macaque). **a**, Naive CD4$^+$ T cells (CD45RA$^+$CD95$^-$) and two subsets of memory CD4$^+$ T cells (CD45RA$^-$, or CD45RA$^+$CD95$^+$) can be identified in tissues of rhesus macaques[6,20]. Before infection, most cells in the blood and lymph nodes are of the naive phenotype; however, acute SIV infection is accompanied by a selective loss of the memory subsets. LN, lymph node. **b**, CCR5 expression is restricted to memory T cells in both CD4$^+$ and CD8$^+$ T cells.

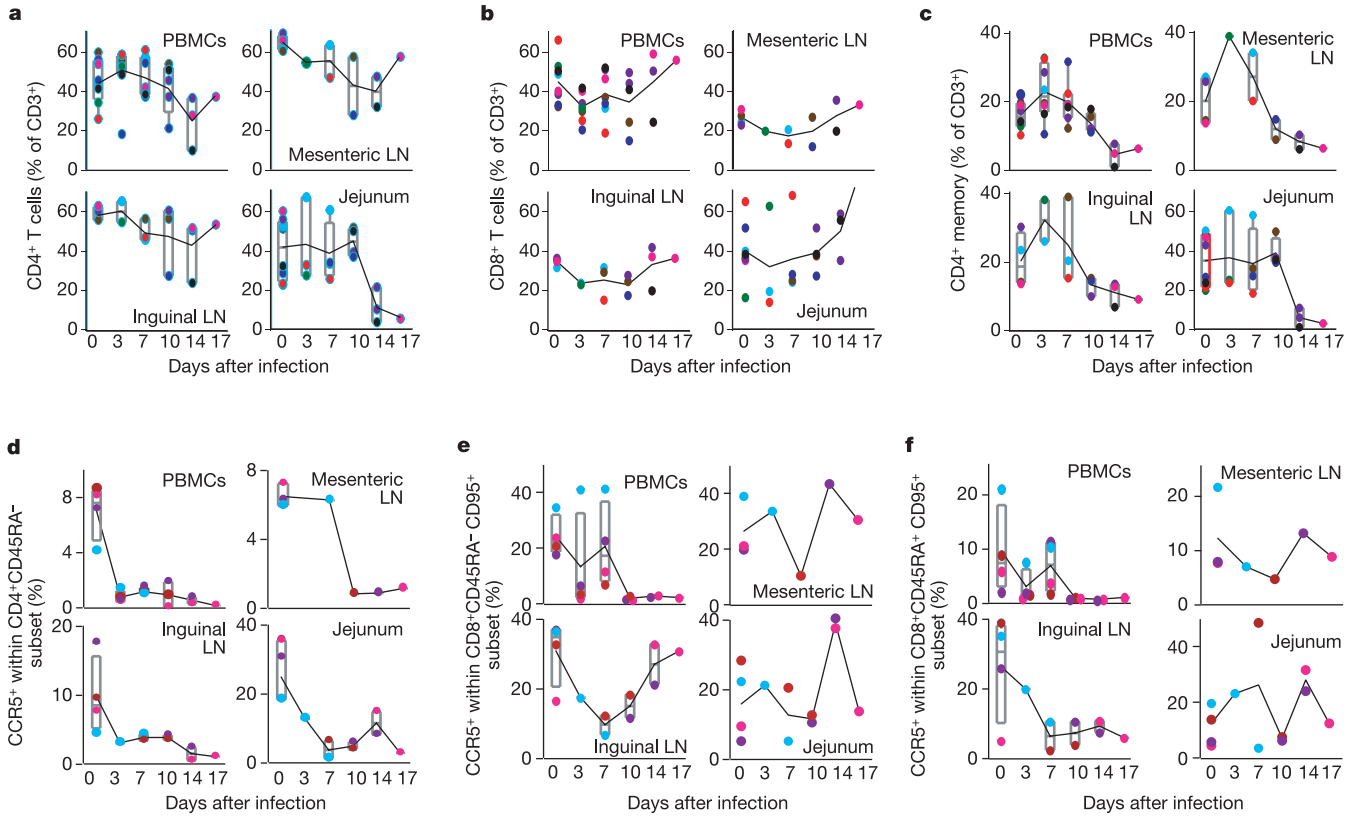

Figure 2 Dynamics of $CD4^+$ and $CD8^+$ subsets during acute SIV infection. **a**, **b**, Modest declines in $CD4^+$ T cells (**a**) occur in all tissues except the jejunum, where a near total loss occurs between days 10 and 14; $CD8^+$ T cells (**b**) show the opposite trend. Nearly all jejunal T cells are of the memory phenotype (Fig. 1b); in other tissues naive T cells predominate. **c**, After an early expansion of $CD4^+$ memory T cells ($CD45RA^+$ and $CD45RA^-$ subsets), most are lost in the subsequent week. *y*-axis values in **a**–**c** are a percentage of total T cells. **d**, $CCR5^+$ $CD4^+$ T cells show early changes, before the onset of detectable viraemia. The percentages are as a fraction of $CD45RA^-$ memory T cells; the fraction within total $CD4^+$ T cells is two- to fourfold lower (Fig. 1b). **e**, **f**, $CCR5^+$ $CD8^+$ T cells also show changes in their response to the SIV challenge, for both the $CD45RA^-$ (**e**) and $CD45RA^+$ (**f**) memory subsets, including a selective loss from blood. These changes illustrate the capacity of $CCR5^+$ T cells to redistribute in the body, limiting interpretations of the loss of these cells from measurements solely on blood. Boxes represent interquartile range, where applicable. Within this figure, colours identify individual animals.

$CCR5^+$ memory cells (Fig. 4; sorted cells were >99% pure). $CCR5^-$ memory cells had ~20-fold more mRNA than naive T cells; similarly they had ~20-fold less than $CCR5^+$ memory T cells. Thus, many '$CCR5^-$' memory T cells may in fact express sufficient levels of CCR5 to render them susceptible to SIV infection—as was shown *in vitro* for HIV infection[16]. An alternative explanation is that CCR5 expression is highly labile and does not preclude the possibility that infected cells were $CCR5^+$ at the time they were infected. In any case, CCR5 expression on $CD4^+$ memory T cells, measured at a single time point, cannot be used to describe viral dynamics accurately.

Discussion

We find that acute SIV infection is accompanied by a surprisingly high rate of infection and subsequent deletion of memory $CD4^+$ T cells, across a wide spectrum of tissues in the host. Previous estimates of the infection rate of $CD4^+$ T cells were well under 1% (refs 7–10). The markedly higher levels of infection that occur during acute viraemia last only a few days: after the peak, at which 30–60% of all memory $CD4^+$ T cells are infected, the cell-associated viral loads drop very rapidly. Indeed, during the first 4 days after peak, we found that about 80% of infected cells are eliminated, either by virus-induced cytolysis, or by an immune-

Table 1 **Quantification of SIV infection at the single cell level**

Tissue	Gag copies per cell*	Infection rate (%)†		
		10 cells per well	30 cells per well	100 cells per well
PBMCs	1.45	29	30	31
Mesenteric lymph nodes	1.51	57	50	55
Jejunum	1.61	59	60	62
Inguinal lymph nodes	1.45	44	44	59

*For each tissue (day 10 after infection), single $CD4^+$ memory T cells were deposited in 72 wells by a flow cytometer. The average signal from the positive wells was converted to Gag copies per cell based on a calibration using a cell line with a single integrated virion. The efficiency of recovering PCR signal from the cell line was 77%.
† A total of 12–36 wells, each containing 10, 30, or 100 cells deposited by a flow cytometer, were quantified for SIV-Gag DNA; the resulting signal was divided by the average number of copies per cell (second column) to define the fraction of infected cells. This percentage correlates very well with the values obtained from the bulk qPCR analyses (see Fig. 3), for which the cell number was calculated from albumin DNA qPCR.

mediated mechanism. Because 30–60% of all memory CD4$^+$ T cells were infected, this corresponds to an elimination of 24–48% of all memory T cells between day 10 and day 14. Loss of memory CD4$^+$ T cells continues after day 14, albeit to a lesser extent.

The loss of infected cells measured by qPCR (Fig. 3b) corresponds with the loss of memory CD4$^+$ T cells measured phenotypically (Fig. 2c). Thus, we can explain the loss of CD4$^+$ memory T cells during acute infection solely by mechanisms related to the direct infection of these cells by SIV: either by SIV-induced cytolysis or an SIV-specific immune response that kills the infected cells. No 'bystander' killing mechanisms need be invoked to account for the observed T-cell dynamics, although we cannot rule out that such mechanisms still occur.

The rapidity and extent with which peak viraemia is achieved and resolved makes detailed measurement of viral and T-cell dynamics particularly difficult. In order to derive the best measurements for quantitative kinetic analysis, nearly daily sampling may be necessary. In addition, when modelling phenotype-defined dynamics, it is important to consider that there are many changes occurring in peripheral blood well before the onset of viraemia (Fig. 2), suggesting that the acute innate immune response is affecting lymphocyte trafficking. Such dynamics have not been considered in the modelling of the acute infection and may markedly affect the interpretations of such models.

The fact that most memory T cells can be infected is not unexpected: lentiviruses are known to infect non-cycling cells, and resting memory T cells have been shown to harbour SIV[17,18]. However, the efficient depletion of infected cells at days 10–14 means that the infection of these cells must be accompanied by at least a minimal expression of viral genes. The selective depletion of the infected cells is due to either CD8-mediated killing (requiring sufficient expression of viral genes to render the infected cells 'visible' to cytotoxic T lymphocytes) or a viral-induced cytopathic event involving some level of cellular activation. In any case, our observations demonstrate that most memory CD4$^+$ T cells can support a sufficiently productive infection, leading to their demise.

The extent to which memory CD4$^+$ T cells could be infected during the acute stage was a surprise. Why is it that the fraction of infected cells at the chronic stage is so low ($\ll$1%; refs 7–10)? Clearly the immune response is dramatically affecting the balance in the chronic phase, and perhaps the viruses produced at later stages contain a much greater proportion of non-infectious particles. It is remarkable that, even at late stages, in the presence of relatively high amounts of virus (10^4 virions per ml), only a small proportion of the susceptible memory CD4$^+$ T-cell population carries virus.

We found that naive CD4$^+$ T cells are highly (or completely) resistant to SIV infection (Fig. 3b), in agreement with a previous study[15]. As a consequence, the dynamics of peripheral blood CD4$^+$ T cells is highly tempered because of the presence of a large (and variable) fraction of these resistant cells: the massive depletion of the memory compartment is masked by the majority of the population (naive T cells) that is unaffected by SIV. We recommend that future

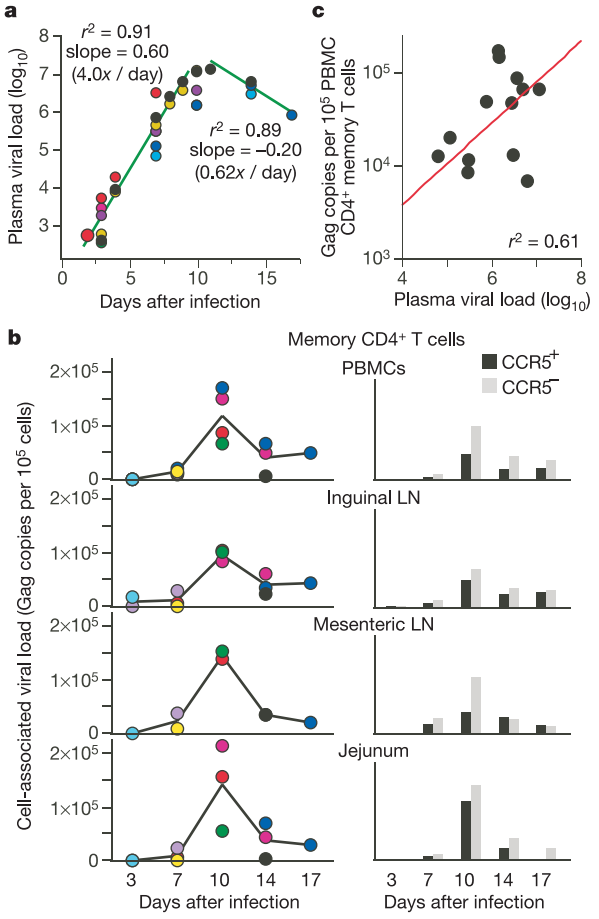

Figure 3 Viral dynamics during acute infection. **a**, Plasma virus was first detected at day 3 after infection and peaked at day 10, at 10^7 copies per ml. Note that animals were killed at various times throughout the time course. A least-squares (log-linear) regression of the rise and fall in viral loads is shown. **b**, Cell-associated viral loads for sorted memory CD4$^+$ T cells. The peak in cell-associated viral load coincided with the plasma viral load (day 10 after infection), and fell as much as 80% by day 14. CCR5$^+$ and CCR5$^-$ memory CD4$^+$ T cells were sorted from these tissues; the average viral load for the two subsets is shown in the bar charts. **c**, The plasma viral load is reasonably well correlated with the memory CD4$^+$ T-cell-associated viral load.

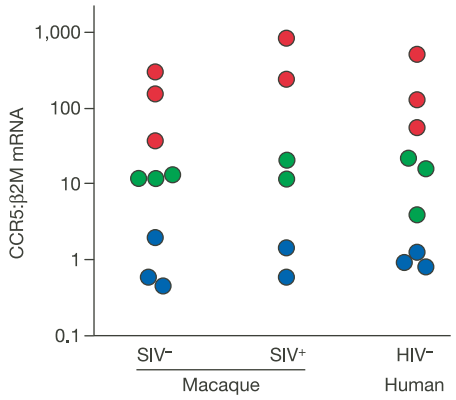

Figure 4 Expression of CCR5 mRNA by T cells. Quantitative RT–PCR was used to compare the CCR5 mRNA levels in sorted CD4$^+$ naive (blue), CCR5$^+$ memory (red) and CCR5$^-$ memory (green) T cells in three SIV-negative macaques, two SIV-positive macaques (at day 10 after infection) and three HIV-negative humans.

Table 2 **Tissue sampling schedule**

Number of animals	Blood (day)	Jejunum (day)	Inguinal lymph nodes (day)	Mesenteric lymph nodes (day)
1	P, 0, 3	P, 0, 3	P, 0, 3	P, 3
2	P, 0, 3, 7	P, 3, 7	P, 3, 7	P, 7
2	P, 0, 3, 7, 10	P, 7, 10	P, 7, 10	P, 10
2	P, 0, 3, 7, 10, 14	P, 10, 14	P, 10, 14	P, 14
1	P, 0, 3, 7, 10, 14, 17	P, 14, 17	P, 14, 17	P, 17

Listed are the days after infection (where P indicates 1 month before infection) at which samples were collected from each animal in the group. The last collection date was a necropsy; all animals sustained only a single survival surgery.

studies of SIV T-cell dynamics (and, for example, evaluation of vaccine efficacy) be tailored to longitudinally distinguish naive and memory $CD4^+$ T cells—the animal-to-animal variation in the naive/memory balance could mask clinically important changes in the memory $CD4^+$ T cells.

Acute SIV infection is considerably more marked than has been previously described. There is an extensive loss of memory $CD4^+$ T cells not only from mucosal tissues (where most $CD4^+$ T cells reside) but also from organized lymph nodes and peripheral blood. The high rate of infection of these T cells is a sufficient mechanism to account for their loss during acute infection; no bystander mechanisms need be invoked. It is clear that a central aim for effective vaccines (or early intervention drug therapy) must be to prevent this massive destruction of the $CD4^+$ memory compartment by tempering the cell-associated viral load at the peak time point. □

Methods

Animals, infection and samples

Eight colony-bred healthy rhesus macaques (*Macaca mulatta*) housed at Bioqual Inc were used in this study. Animals were housed in accordance with American Association for Accreditation of Laboratory Animal Care guidelines and were sero-negative for SIV, simian retrovirus and simian T-cell leukaemia virus type-1. Animals were infected with 100 animal infectious doses of uncloned pathogenic SIVmac251 intravenously (courtesy of N. Letvin); plasma and tissue samples were collected at various time points by biopsy or necropsy (Table 2).

Tissue sampling

Peripheral blood mononuclear cells (PBMCs) were isolated by density gradient centrifugation. Jejunal biopsy and necropsy samples were isolated as previously described[2]. Lymph node cell suspensions were made by pushing tissue through a small-gauge syringe needle. Plasma viral RNA levels were determined by real-time PCR (ABI Prism 7700 sequence detection system, Applied Biosystems) using reverse-transcribed viral RNA as templates, as described[19].

Antibodies and flow cytometry

All antibodies were purchased from PharMingen, either conjugated or unconjugated and derivatized in our laboratory. All reagents were validated and titrated using rhesus macaque PBMCs. For phenotypic analysis, freshly isolated cells were labelled simultaneously with the following combinations of antibodies: CD3-Cy7-allophycocyanin (APC), CD8-Cy5.5-phycoerythrin (PE), CD4-cascade blue, CD45RA-TRPE, CD95-APC, CCR5-PE. Labelled cells were fixed with 0.5% paraformaldehyde and analysed using a modified Becton Dickinson Digital Vantage. At least one million total events were collected. To determine which subsets supported viral infection, naive and memory $CD4^+$ T cells (discriminated on the basis of CD45RA and CD95 expression[20]) were sorted into tubes and subjected to qPCR assay for measuring SIV-Gag DNA[7]. To determine whether these T-cell subsets harboured single or multiple copies of SIV-Gag DNA, cells were sorted directly into 96-well PCR plates at varying frequencies of 1–100 cells per well and subjected to qPCR analysis. For each sort, a cell line containing a single copy of proviral SIV DNA (described below) was also sorted to validate the qPCR assay.

qPCR assay for SIV-Gag DNA

T-cell-associated viral DNA was measured by a quantitative PCR assay for SIV *gag* using a Perkin-Elmer ABI 7700 instrument as previously described[7], and using SIV *gag* primers and probe as described previously[21].

Quantification of CCR5 mRNA

T-cell subsets were sorted directly into *RNA*later (Ambion Inc.) and centrifuged at 10,000*g* for 3 min. Supernatants were discarded and total RNA was extracted using RNAqueous-4-PCR and treated with 2 units of DNase for 30 min at 37 °C (Ambion Inc.). After DNase treatment, mRNA was purified using the Oligotex mRNA extraction kit as per the manufacturer's instructions (Qiagen).

Purified mRNA was added directly to a one-step quantitative RT–PCR reaction containing Superscript RT-Platinum Taq enzyme mix (Invitrogen). CCR5 and normalizing gene probes (β2-microglobulin, or β2M) were labelled with a 5′ FAM reporter and 3′ BHQ1 quencher (Biosource). We used the following oligonucleotide sequences: CCR5 forward primer, GTCCCCTTCTGGGCTCACTAT; CCR5 reverse primer, CCCTGTCAAGAGTTGACACATTGTA; CCR5 probe, FAM-TCCAAAGTCCCACTGGGCAGCAG-BHQ1; β2M forward primer, GCTGGCGCT ACTCTCTCTTTCT; B2M reverse primer, GGATGGCGTGAGTAAACCTGAA; B2M probe, FAM-CCTGGAGGCTATCCAGCGTACTCCAAAG-BHQ1. Expression levels of human and non-human primate CCR5 were normalized to β2-microglobulin and calculated based on the $\Delta\Delta C_T$ method[22]; Fig. 4 shows the values normalized to the average value for naive $CD4^+$ T cells in each group.

Generation of a cell line with a single copy of SIV proviral DNA

CEM x174 cells were infected with SIVmac316 (ref. 23) at a multiplicity of infection of 0.01. As previous studies had shown that cultured cells surviving acute infection harbour low copy numbers of integrated and defective proviral DNA[24], cells were collected 8 weeks after inoculation. Single cells were sorted into 96-well round-bottom plates; a total of 76 clones containing proviral DNA was obtained from 384 individual wells. Southern blotting of restricted genomic DNA was performed to determine the copy number(s) of SIV proviral DNA in each cell, as previously reported[25]. Three clones (2A7, 2E10 and 3D8), each containing a single copy of SIV DNA, were identified; clone 3D8 was used in this study. This clone produces no detectable virus.

Data analysis

Flow cytometric data were analysed using FlowJo version 6.1 (Tree Star, Inc.). Statistical analyses were computed with JMP (SAS Institute).

Received 22 December 2004; accepted 25 February 2005; doi:10.1038/nature03501.
Published online 27 March 2005.

1. Veazey, R. S. *et al.* Gastrointestinal tract as a major site of $CD4^+$ T cell depletion and viral replication in SIV infection. *Science* **280,** 427–431 (1998).
2. Mattapallil, J. J., Smit-McBride, Z., McChesney, M. & Dandekar, S. Intestinal intraepithelial lymphocytes are primed for γ-interferon and MIP-1β expression and display antiviral cytotoxic activity despite severe $CD4^+$ T-cell depletion in primary simian immunodeficiency virus infection. *J. Virol.* **72,** 6421–6429 (1998).
3. Brenchley, J. M. *et al.* $CD4^+$ T cell depletion during all stages of HIV disease occurs predominantly in the gastrointestinal tract. *J. Exp. Med.* **200,** 749–759 (2004).
4. Veazey, R. S. *et al.* Dynamics of CCR5 expression by $CD4^+$ T cells in lymphoid tissues during simian immunodeficiency virus infection. *J. Virol.* **74,** 11001–11007 (2000).
5. Veazey, R. S. *et al.* Identifying the target cell in primary simian immunodeficiency virus (SIV) infection: highly activated memory $CD4^+$ T cells are rapidly eliminated in early SIV infection *in vivo*. *J. Virol.* **74,** 57–64 (2000).
6. Mattapallil, J. J., Letvin, N. L. & Roederer, M. T-cell dynamics during acute SIV infection. *AIDS* **18,** 13–23 (2004).
7. Douek, D. C. *et al.* HIV preferentially infects HIV-specific $CD4^+$ T cells. *Nature* **417,** 95–98 (2002).
8. Haase, A. T. *et al.* Quantitative image analysis of HIV-1 infection in lymphoid tissue. *Science* **274,** 985–989 (1996).
9. Haase, A. T. Population biology of HIV-1 infection: viral and $CD4^+$ T cell demographics and dynamics in lymphatic tissues. *Annu. Rev. Immunol.* **17,** 625–656 (1999).
10. Lassen, K., Han, Y., Zhou, Y., Siliciano, J. & Siliciano, R. F. The multifactorial nature of HIV-1 latency. *Trends Mol. Med.* **10,** 525–531 (2004).
11. Chen, Z., Zhou, P., Ho, D. D., Landau, N. R. & Marx, P. A. Genetically divergent strains of simian immunodeficiency virus use CCR5 as a coreceptor for entry. *J. Virol.* **71,** 2705–2714 (1997).
12. Marcon, L. *et al.* Utilization of C–C chemokine receptor 5 by the envelope glycoproteins of a pathogenic simian immunodeficiency virus, SIVmac239. *J. Virol.* **71,** 2522–2527 (1997).
13. Jung, A. *et al.* Multiply infected spleen cells in HIV patients. *Nature* **418,** 144 (2002).
14. Gratton, S., Cheynier, R., Dumaurier, M. J., Oksenhendler, E. & Wain-Hobson, S. Highly restricted spread of HIV-1 and multiply infected cells within splenic germinal centers. *Proc. Natl Acad. Sci. USA* **97,** 14566–14571 (2000).
15. Nishimura, Y. *et al.* Highly pathogenic SHIVs and SIVs target different $CD4^+$ T cell subsets in rhesus monkeys, explaining their divergent clinical courses. *Proc. Natl Acad. Sci. USA* **101,** 12324–12329 (2004).
16. Mengozzi, M. *et al.* Naive CD4 T cells inhibit CD28-costimulated R5-tropic HIV replication in memory CD4 T cells. *Proc. Natl Acad. Sci. USA* **98,** 11644–11649 (2001).
17. Zhang, Z. *et al.* Sexual transmission and propagation of SIV and HIV in resting and activated $CD4^+$ T cells. *Science* **286,** 1353–1357 (1999).
18. Zhang, Z. Q. *et al.* Roles of substrate availability and infection of resting and activated $CD4^+$ T cells in transmission and acute simian immunodeficiency virus infection. *Proc. Natl Acad. Sci. USA* **101,** 5640–5645 (2004).
19. Endo, Y. *et al.* Short- and long-term clinical outcomes in rhesus monkeys inoculated with a highly pathogenic chimeric simian/human immunodeficiency virus. *J. Virol.* **74,** 6935–6945 (2000).
20. Pitcher, C. J. *et al.* Development and homeostasis of T cell memory in rhesus macaque. *J. Immunol.* **168,** 29–43 (2002).
21. Lifson, J. D. *et al.* Role of $CD8^+$ lymphocytes in control of simian immunodeficiency virus infection and resistance to rechallenge after transient early antiretroviral treatment. *J. Virol.* **75,** 10187–10199 (2001).
22. Livak, K. J. & Schmittgen, T. D. Analysis of relative gene expression data using real-time quantitative PCR and the ΔΔCT Method. *Methods* **25,** 402–408 (2001).
23. Mori, K., Ringler, D. J., Kodama, T. & Desrosiers, R. C. Complex determinants of macrophage tropism in env of simian immunodeficiency virus. *J. Virol.* **66,** 2067–2075 (1992).
24. Folks, T. M. *et al.* Biological and biochemical characterization of a cloned Leu-3- cell surviving infection with the acquired immune deficiency syndrome retrovirus. *J. Exp. Med.* **164,** 280–290 (1986).
25. Folks, T. *et al.* Characterization of a continuous T-cell line susceptible to the cytopathic effects of the acquired immunodeficiency syndrome (AIDS)-associated retrovirus. *Proc. Natl Acad. Sci. USA* **82,** 4539–4543 (1985).

Acknowledgements We thank R. Koup for critical comments on the manuscript; S. Perfetto, J. Yu, R. Nguyen, D. Ambrozak and other members of the VRC Laboratory of Immunology for advice and technical help; M. St Claire for assistance with the animals; and S. Rao, V. Dang and J.-P. Todd for their assistance during the course of this study.

Competing interests statement The authors declare that they have no competing financial interests.

Correspondence and requests for materials should be addressed to M.R. (Roederer@nih.gov).